

Microscopic theory of temperature-dependent magnetoelectric effect in Cr_2O_3

Maxim Mostovoy,¹ Andrea Scaramucci,¹ Kris T. Delaney,² and Nicola A. Spaldin²

¹*Zernike Institute for Advanced Materials, University of Groningen, Nijenborgh 4, The Netherlands*

²*Materials Department, University of California, Santa Barbara, California 93106-5050, USA*

(Dated: October 31, 2018)

We calculate the temperature-dependent magnetoelectric response of Cr_2O_3 from first principles. The form of the dominant magnetoelectric coupling is determined using symmetry arguments, its strength is found using *ab initio* methods, and the temperature dependence of the response is obtained from Monte Carlo simulations. The quantitative agreement of our results with experiment shows that the strong temperature dependence of the magnetoelectric effect in Cr_2O_3 results from non-relativistic exchange interactions and spin fluctuations.

PACS numbers: 75.85.+t, 75.10.Hk, 75.30.Et, 71.15.Mb

Introduction: Recent progress in understanding the subclass of multiferroics in which improper ferroelectric polarizations are induced by non-centrosymmetric magnetic orderings has led to a clarification of the microscopic origins for magnetoelectric coupling.¹ In particular two distinct coupling mechanisms have been identified. The first arises from relativistic effects linking electron spin and orbital momentum, resulting in the antisymmetric $\mathbf{S}_1 \times \mathbf{S}_2$ interaction between spins of magnetic ions. The dependence of the strength of this Dzyaloshinskii-Moriya interaction on polar displacements of ions makes magnets with non-collinear spiral orders ferroelectric.²⁻⁵ In the second mechanism, polar deformations of the lattice are induced by Heisenberg spin exchange interactions $\mathbf{S}_1 \cdot \mathbf{S}_2$, originating from the Fermi statistics of electrons.^{6,7} This non-relativistic mechanism can give rise to stronger magnetoelectric couplings than those resulting from relativistic effects, which tend to be relatively weak in $3d$ transition metal compounds, and is not restricted to non-collinear spin arrangements. Indeed, the electric polarizations of the orthorhombic manganite $\text{Y}_{1-x}\text{Lu}_x\text{MnO}_3$ ⁸ and orthoferrite GdFeO_3 ,⁹ which have collinear antiferromagnetic spin orderings and polarization arising from the Heisenberg mechanism, exceed the largest polarizations observed in spiral multiferroics by one order of magnitude.

In this work we show that, in addition to causing multiferroic behavior, the relativistic and Heisenberg exchange mechanisms can both give rise to the linear magnetoelectric effect, in which an applied magnetic field induces an electric polarization proportional to the field and, conversely, magnetization is induced by an applied electric field (for a review see Ref.10). Furthermore, the two mechanisms can co-exist in the same material and dominate in different temperature regimes. Using a combination of first-principles density functional theory and Monte Carlo methods we calculate the temperature-dependent magnetoelectric response of the prototype magnetoelectric material, chromium sesquioxide, Cr_2O_3 . We show that the strong finite-temperature magnetoelectric response originates from the Heisenberg exchange mechanism combined with thermal spin fluctuations, whereas at zero temperature, where spin fluctuations

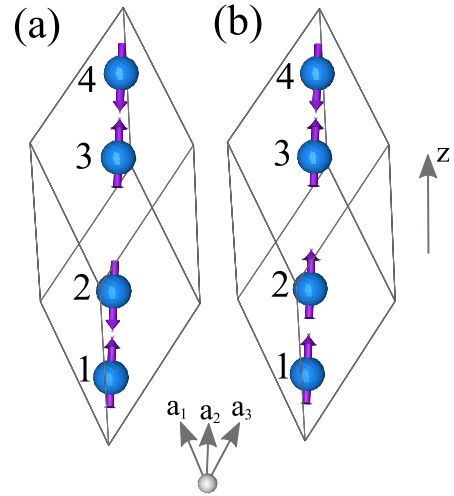


FIG. 1: (Color online) Rhombohedral unit cell of Cr_2O_3 with the unit vectors \mathbf{a}_i , $i = 1, 2, 3$, containing four magnetic Cr ions. Panel (a) shows the actual antiferromagnetic spin ordering in Cr_2O_3 , while panel (b) shows the spin ordering imposed in our first-principle calculations to induce an electric polarization along the trigonal z axis.

vanish, the observed weak response arises from relativistic effects. Significantly, Cr_2O_3 is a collinear antiferromagnet, and so our work extends the recent suggestion that Heisenberg exchange interactions can give rise to a strong magnetoelectric effect in frustrated magnets in which spins are forced to form non-collinear orders with nonzero toroidal or monopole moments.^{11,12}

Magnetoelectric coupling: The magnetoelectric effect in Cr_2O_3 was predicted phenomenologically by Dzyaloshinskii¹³ and measured by Astrov¹⁴ shortly after the theoretical prediction. Cr_2O_3 has four Cr^{3+} ions with spin $S = 3/2$ in the rhombohedral unit cell. Below $T_N = 307\text{K}$ it shows collinear $\uparrow\downarrow\uparrow\downarrow$ spin ordering along the trigonal z axis¹⁵ [see Fig. 1 (a)]. This antiferromagnetic ordering preserves the three-fold and two-fold symmetry axes of the paramagnetic phase, but it breaks inversion symmetry I , reducing it to I' (inversion combined with

time reversal), which allows for two independent magnetoelectric coupling terms in the free energy¹³:

$$F_{\text{me}} = -g_{\parallel} G^z E^z H^z - g_{\perp} G^z (E^x H^x + E^y H^y), \quad (1)$$

where $G^z = \langle S_1^z - S_2^z + S_3^z - S_4^z \rangle$ is the antiferromagnetic order parameter. The two magnetoelectric coefficients, $\alpha_{\parallel} = g_{\parallel} G^z$ and $\alpha_{\perp} = g_{\perp} G^z$, show very different temperature dependences.¹⁴ While α_{\perp} varies only in the immediate vicinity of the transition temperature, T_N , the coefficient α_{\parallel} is very strongly temperature dependent. α_{\parallel} reaches its maximum at $T_{\text{max}} \sim 260\text{K}$, below which it steeply decreases and changes sign at $\sim 100\text{K}$. While at T_{max} the magnitude of α_{\parallel} is one order of magnitude larger than $|\alpha_{\perp}|$, at low temperatures $|\alpha_{\parallel}| < |\alpha_{\perp}|$.

Early measurements of the temperature dependence of the magnetoelectric coefficients,¹⁶⁻¹⁸ as well as recent first-principles calculations,¹⁹ show that the relatively weak magnetoelectric effects at low temperature result from relativistic interactions. In what follows, we demonstrate that the much stronger response at elevated temperatures originates from Heisenberg exchange.

Phenomenologically, the coupling of the electric polarization P^z along the trigonal axis to spins, resulting from the dependence of spin-exchange constants on polar lattice distortions, is described by

$$P^z = \lambda (\mathbf{S}_1 \cdot \mathbf{S}_3 - \mathbf{S}_2 \cdot \mathbf{S}_4), \quad (2)$$

where \mathbf{S}_{α} with $\alpha = 1, 2, 3, 4$ denotes the sublattice magnetization and λ is the coupling strength that we will determine from *ab initio* calculations. Here we take into account the fact that the exchange-driven polarization can only depend on scalar products of the magnetizations. The combination of scalar products in the right-hand side of Eq.(2) transforms as P^z , which changes sign under C_2 and I . The combination of scalar products that lead to this property can be seen by inspection of Table I, which shows how the four inequivalent magnetic sites transform under the symmetry operations of Cr_2O_3 .

	C_3	C_2	I
1	1	2	4
2	2	1	3
3	3	4 - c	2
4	4	3 - c	1

TABLE I: Transformation of four independent Cr sites with the fractional coordinates $\mathbf{r}_1 = (u, u, u)$, $\mathbf{r}_2 = (1/2 - u, 1/2 - u, 1/2 - u)$, $\mathbf{r}_3 = (1/2 + u, 1/2 + u, 1/2 + u)$, and $\mathbf{r}_4 = (1 - u, 1 - u, 1 - u)$, where $u \approx 0.153$, under the generators of space group $R\bar{3}c$: the 120° -rotation around the z axis, $C_3 = (x_3, x_1, x_2)$, the 180° -rotation around the axis orthogonal to the z -direction, $C_2 = (1/2 - x_2, 1/2 - x_1, 1/2 - x_3)$ and inversion $I = (1 - x_1, 1 - x_2, 1 - x_3)$. Here, $\mathbf{c} = \mathbf{a}_1 + \mathbf{a}_2 + \mathbf{a}_3$, where \mathbf{a}_i ($i = 1, 2, 3$) are the rhombohedral unit vectors.

Equation (2) is clearly appropriate for describing electric polarization induced by spin ordering in a multiferroic material. In addition, it applies to the linear

magnetoelectric effect, as can be seen from the following heuristic argument: In an applied magnetic field H^z the average value of spin on the sublattice α changes by $\langle \delta S_{\alpha}^z \rangle \propto \chi_{\parallel} H^z$, where χ_{\parallel} is the longitudinal magnetic susceptibility. Equation (2) then gives $P^z \propto \lambda \chi_{\parallel} \langle S_1^z - S_2^z + S_3^z - S_4^z \rangle H^z \propto G^z H^z$, consistent with $P^z = -\frac{\partial F_{\text{me}}}{\partial E^z} = g_{\parallel} G^z H^z$ obtained from Eq.(1).

Equation (2) is only meaningful within the mean field approach. To account for effects of spin fluctuations on the magnetoelectric response of Cr_2O_3 we will use the microscopic expression for the exchange-driven polarization in terms of scalar products of Cr spins (rather than the sublattice magnetizations), which has the form

$$P^z = \frac{\lambda}{6N} \sum_j \sum_{n=1}^6 (\mathbf{S}_{1,j} \cdot \mathbf{S}_{3,j-b_n} - \mathbf{S}_{2,j} \cdot \mathbf{S}_{4,j-b_n}). \quad (3)$$

Here j labels unit cells, N is the total number of unit cells, and $\mathbf{b}_1 = \mathbf{a}_1$, $\mathbf{b}_2 = \mathbf{a}_2$, $\mathbf{b}_3 = \mathbf{a}_3$, $\mathbf{b}_4 = \mathbf{a}_1 + \mathbf{a}_2$, $\mathbf{b}_5 = \mathbf{a}_2 + \mathbf{a}_3$, $\mathbf{b}_6 = \mathbf{a}_3 + \mathbf{a}_1$ (\mathbf{a}_i being the rhombohedral unit vectors). Remarkably, the interaction between the fourth nearest-neighbor Cr ions separated by the distance $r_{1,(3-a_1)} = r_{1,(3-a_1-a_2)} = 3.65\text{\AA}$ turns out to give rise to the magnetoelectric effect in Cr_2O_3 . The shorter-range exchange interactions do not couple the sublattices 1 and 3 (or 2 and 4) and, therefore, do not contribute to P^z , while other interactions between these sublattices correspond to much longer exchange paths and are negligibly small. This allows us to accurately pinpoint the microscopic origin of the strong magnetoelectric effect in Cr_2O_3 .

Importantly, Eqs.(2) and (3) apply to any four-sublattice spin ordering in Cr_2O_3 . The $\uparrow\downarrow\uparrow\downarrow$ spin ordering realized in the low-temperature ground-state of Cr_2O_3 induces no electric polarization, and so a straightforward density-functional study of Cr_2O_3 does not give information about the strength of the finite-temperature perpendicular magnetoelectric coupling. However, the $\uparrow\uparrow\downarrow$ ordering shown in Fig. 1 (b) renders Cr_2O_3 multiferroic and induces the electric polarization

$$\mathcal{P} \equiv P^z(\uparrow\uparrow\downarrow) = 2\lambda S^z. \quad (4)$$

We next extract λ using *ab initio* methods by enforcing $\uparrow\uparrow\downarrow$ spin ordering and calculating the magnetically-induced polarization \mathcal{P} .

First-principles calculations of the magnetoelectric coupling: We compute λ and the spin exchange parameters using plane-wave density-functional theory, as implemented in the Vienna Ab-initio Simulation Package (VASP).²⁰ We use PAW potentials²¹ for core-valence partitioning, and the local-spin-density approximation with a rotationally invariant Hubbard- U (LSDA+ U) for the exchange-correlation potential.²⁶ Our Hubbard $U = 2.0\text{eV}$ is the same value that was taken for computing the magnetoelectric response at zero temperature.¹⁹ We deliberately do not include spin-orbit coupling, and all calculations are for collinear spin densities, so that λ

corresponds only to polarizations induced by exchange striction.

We find that a plane-wave cutoff of 500 eV and Monkhorst-Pack²² k -point sampling of $4 \times 4 \times 4$ are sufficient for computing the properties of interest. Note that much finer k meshes would be required for accurately resolving the magnetocrystalline easy axis,¹⁹ but non-relativistic properties are well converged with our chosen parameters.

We work with space group $R\bar{3}c$ at the experimental volume²³ of 96.0 \AA^3 and rhombohedral angle of 55.13° . The internal coordinates are relaxed within our density functional calculations for the $\uparrow\downarrow\uparrow\downarrow$ magnetic configuration, yielding coordinates $x = 0.1536$ for Cr, and $x = 0.9426$ for O in Wyckoff positions $4c$ and $6e$ respectively. Subsequently, the Heisenberg exchange couplings $J_1 - J_5$,²⁴ corresponding to Cr-Cr distances of 2.65 to 4.10 \AA , are computed by fitting a Heisenberg Hamiltonian to DFT total energies of twelve different spin configurations with fixed ion coordinates in the hexagonal setting of $R\bar{3}c$. This method is analogous to that employed by Shi *et al.*²⁵

Finally, we compute λ by enforcing the spin configuration of $\uparrow\uparrow\uparrow\downarrow$ and re-relaxing the ionic coordinates in the rhombohedral unit cell. The resulting ionic configuration has a polar lattice distortion. We compute the magnitude of $\mathcal{P} = 0.585 \mu\text{C}/\text{cm}^2$ using the Berry phase approach,²⁷ which allows us to extract λ . We note that \mathcal{P} is of the same order of magnitude as the polarization induced by exchange interactions in multiferroics with collinear spins.^{8,9}

Monte Carlo simulations: Using Eq.(3) we can express the magnetoelectric coefficient α_{\parallel} in terms of spin correlation functions:

$$\alpha_{\parallel} = \left. \frac{\partial \langle P^z \rangle}{\partial H^z} \right|_{H^z=0} = \frac{2\mu_B}{k_B T} \langle P^z \sum_{\alpha,j} S_{\alpha,j}^z \rangle, \quad (5)$$

where $\langle \dots \rangle$ denotes the thermal average at temperature T , k_B is the Boltzmann constant and μ_B is the Bohr magneton.

In the mean-field approximation, equivalent to replacing the scalar products of spins $\mathbf{S}_{\alpha,j} \cdot \mathbf{S}_{\beta,k}$ by $\langle \mathbf{S}_{\alpha,j} \rangle \cdot \mathbf{S}_{\beta,k} + \mathbf{S}_{\alpha,j} \cdot \langle \mathbf{S}_{\beta,k} \rangle$ in the expression for P^z , one obtains^{16,17}

$$\alpha_{\parallel} = \frac{\lambda v_0 G^z \chi_{\parallel}}{8\mu_B}, \quad (6)$$

where v_0 is the unit cell volume, in agreement with the simple argument given above. The mean-field expression qualitatively explains the observed temperature dependence of α_{\parallel} : It first grows, together with the order parameter G^z , as the temperature drops below T_N , then subsequently decreases and vanishes at $T = 0$, together with the longitudinal magnetic susceptibility χ_{\parallel} .

In Ref.18 an attempt was made to take into account the effects of spin fluctuations using a higher-order decoupling scheme. This approximation fails, however, close to the transition temperature where spin fluctuations are

large. We include spin fluctuations by calculating α_{\parallel} numerically using Monte Carlo simulations of a system of 864 classical spins with exchange constants and the magnetoelectric coupling λ obtained from our first principles calculations, as described above.

Since the correlation function in the right-hand side of Eq.(5) is zero unless a single antiferromagnetic domain is selected, we apply to our finite spin system a weak staggered field along the z axis, $h(-)^{\alpha}$, where $\alpha = 1, 2, 3, 4$ labels magnetic sublattices. This mimics the easy magnetic anisotropy of Cr_2O_3 as well as the cooling in electric and magnetic fields, used in measurements of magnetoelectric coefficients to select the domain with a given sign of magnetic order parameter. The field strength, $h = 0.165 \text{ meV}$, was chosen so that it is small compared to the scale of exchange interactions, but large enough to make the Monte Carlo results independent of h .

Figure 2 shows the temperature dependence of α_{\parallel} obtained from Monte Carlo simulations (blue circles) and in the mean-field approximation described above (red solid line). The onset of the magnetoelectric response in our Monte Carlo simulations, as well as the sharp peak in the specific heat (inset), shows that the antiferromagnetic order sets in at $\sim 290 \text{ K}$, close to the experimentally observed transition temperature $T_N = 307 \text{ K}$. The maximal value of the magnetoelectric coefficient obtained from our simulations is 0.9×10^{-4} (in CGS units), in excellent agreement with the experimental value of 1.0×10^{-4} (see Ref.28). The maximum value is reached at $\sim 240 \text{ K}$ that compares well to $T_{\text{max}} \sim 260 \text{ K}$ found in experiment. The mean field transition temperature (425 K) and maximal α_{\parallel} are significantly higher than the Monte Carlo values, indicating the importance of spin fluctuations in this material.

Conclusions: We have presented the first *ab initio* calculations of temperature-dependent linear magnetoelectric responses. The quantitative agreement of our results with experimental data on Cr_2O_3 demonstrates that the dominant parallel magnetoelectric coupling in this material originates from non-relativistic exchange interactions between electrons. The strong temperature dependence of the magnetoelectric coefficient α_{\parallel} underscores the general importance of spin fluctuations for magnetoelectric responses of materials with collinear spin orders. The magnetic-field-induced electric polarization of Cr_2O_3 is comparable to that predicted recently for an exchange-interaction-driven Kagome antiferromagnet with non-collinear spin ordering.¹¹ However, the magnetoelectric response of non-collinear magnets does not vanish at zero temperature as it involves transverse rather than longitudinal magnetic susceptibility and originates from the dynamic ‘electromagnon’ modes, which can be excited by both electric and magnetic fields and which are absent in collinear magnets.^{29,30}

The approach used in this paper, specifically the combination of first principles calculations for artificially imposed magnetic states to extract parameters with Monte Carlo simulations of physically interesting quantities,

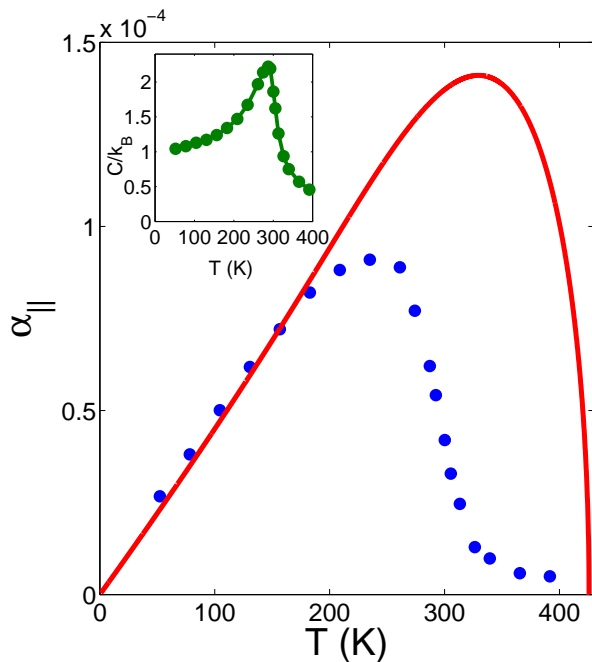


FIG. 2: (Color online) Temperature dependence of the magnetoelectric coupling α_{\parallel} obtained using *ab initio* values of the exchange constants and magnetoelectric coupling combined with Monte Carlo simulations (blue circles) and mean field calculations (solid red line). The inset shows the temperature dependence of magnetic specific heat.

opens a route to theoretical studies of a large variety of temperature-dependent static and dynamic magnetoelectric phenomena. Accurate predictions of the magnitude of magnetoelectric responses at finite temperature will greatly facilitate the search for and design of materials with the strongest responses.

Acknowledgments

The work of MM and AS was supported by the Thrust II program of the Zernike Institute for Advanced Materials and by the Stichting voor Fundamenteel Onderzoek der Materie (FOM). KTD and NAS were supported by the National Science Foundation under Award No. DMR-0940420. This work made use of the computing facilities of the California Nanosystems Institute with facilities provided by NSF grant No. CHE-0321368 and Hewlett-Packard.

- ¹ A review: S.-W. Cheong and M. Mostovoy, *Nature Mater.* **6**, 13 (2007).
- ² H. Katsura, N. Nagaosa, and A.V. Balatsky, *Phys. Rev. Lett.* **95**, 057205 (2005).
- ³ I.A. Sergienko and E. Dagotto, *Phys. Rev. B* **73**, 094434 (2006).
- ⁴ M. Mostovoy, *Phys. Rev. Lett.* **96**, 067601 (2006).
- ⁵ A. Malashevich and D. Vanderbilt, *Phys. Rev. Lett.* **101**, 037210 (2008).
- ⁶ I.A. Sergienko, C. Sen, and E. Dagotto, *Phys. Rev. Lett.* **97**, 227204 (2006).
- ⁷ S. Picozzi, K. Yamauchi, B. Sanyal, I.A. Sergienko, and E. Dagotto, *Phys. Rev. Lett.* **99**, 227201 (2007).
- ⁸ S. Ishiwata, Y. Kaneko, Y. Tokunaga, Y. Taguchi, T. Arima, and Y. Tokura, preprint arXiv:0911.4190.
- ⁹ Y. Tokunaga, N. Furukawa, H. Sakai, Y. Taguchi, T. Arima and Y. Tokura, *Nature Mater.* **8**, 558 (2009).
- ¹⁰ M. Fiebig, *J. Appl. Phys.* **98**, R123 (2005).
- ¹¹ K.T. Delaney, M. Mostovoy, and N.A. Spaldin, *Phys. Rev. Lett.* **102**, 157203 (2009).
- ¹² N.A. Spaldin, M. Fiebig, and M. Mostovoy, *J. Phys.: Condens. Matter* **20**, 434203 (2008).
- ¹³ I.E. Dzyaloshinskii, *Sov. Phys. JETP* **10**, 628 (1959).
- ¹⁴ D.N. Astrov, *Sov. Phys. JETP* **11**, 708 (1960); *ibid.* **13** 729 (1961).
- ¹⁵ B.N. Brockhouse, *J. Chem. Phys.* **21**, 961 (1953).
- ¹⁶ G. Rado, *Phys. Rev.* **128**, 2546 (1962).
- ¹⁷ R. Hornreich and S. Shtrikman, *Phys. Rev. B* **161**, 506 (1967).
- ¹⁸ H. Yatom and R. Englman, *Phys. Rev.* **188** 793 (1969); *ibid.* 803 (1969).
- ¹⁹ J. Íñiguez, *Phys. Rev. Lett.* **101**, 117201 (2008).
- ²⁰ G. Kresse and J. Hafner, *Phys. Rev. B* **48**, 13115 (1993); G. Kresse and J. Furthmüller, *Phys. Rev. B* **54**, 11169 (1996).
- ²¹ P.E. Blöchl, *Phys. Rev. B* **50**, 17953 (1994); G. Kresse and D. Joubert, *Phys. Rev. B* **59**, 1758 (1999).
- ²² H. Monkhorst and J.D. Pack, *Phys. Rev. B* **13**, 5188 (1976).
- ²³ L.W. Finger and R.M. Hazen, *J. Appl. Phys.* **51**, 5362 (1980).
- ²⁴ The exchange constants are labeled as in E.J. Samuelsen, M.T. Hutchings, and G. Shirane, *Physica (Amsterdam)* **48**, 13 (1970).
- ²⁵ S. Shi, A.L. Wysocki, K.D. Belashchenko, *Phys. Rev. B* **79**, 104404 (2009).
- ²⁶ A.I. Liechtenstein, V.I. Anisimov and J. Zaanen, *Phys. Rev. B* **52**, R5467 (1995).
- ²⁷ R.D. King-Smith and D. Vanderbilt, *Phys. Rev. B* **47**, 1651 (1993); D. Vanderbilt and R.D. King-Smith, *Phys. Rev. B* **48**, 4442 (1993).
- ²⁸ A.S. Borovik-Romanov and H. Grimmer, *International Tables for Crystallography*, Vol. D, ed. A. Authier, (Kluwer Academic, Dordrecht, 2003) pp. 105-149.

- ²⁹ R. Valdés Aguilar, M. Mostovoy, A.B. Sushkov, C.L. Zhang, Y.J. Choi, S-W. Cheong, and H.D. Drew, Phys. Rev. Lett. **102**, 047203 (2009).
- ³⁰ A.M. van der Vegte and M. Mostovoy, preprint arXiv:0907.3055